Crystal structure of a dimeric octaheme cytochrome c_3 (M_r 26 000) from *Desulfovibrio desulfuricans* Norway

M Czjzek[1]*, F Guerlesquin[2], M Bruschi[2] and R Haser[1]

Background: The octaheme cytochrome c_3 (M_r 26 000; cc_3) from *Desulfovibrio desulfuricans* Norway is a dimeric cytochrome made up of two identical subunits, each containing four heme groups. It is involved in the redox transfer chain of sulfate-reducing bacteria, which links the periplasmic oxidation of hydrogen to the cytoplasmic reduction of sulfate. The amino-acid sequence of cc_3 shows similarities to that of the tetraheme cytochrome c_3 (M_r 13 000; c_3) from the same bacteria. Structural analysis of cc_3 forms a basis for understanding the precise roles of the multiheme-containing redox proteins and the reason for the presence of several different multiheme cytochromes in one bacterial strain.

Results: The crystal structure of cytochrome cc_3 has been determined at 2.16 Å resolution. The subunits display the c_3 structural fold with significant amino-acid substitutions, relative to the tetraheme cytochromes c_3, in the regions of the dimer interface. The identical subunits are related by a crystallographic twofold axis, with one heme of each subunit in close contact. The overall structure and the environments of the different heme groups are compared with those of the tetraheme cytochromes c_3.

Conclusions: A common scheme for interactions between these types of cytochrome and their redox partners involves the interaction of a heme crevice, surrounded by positively charged lysine residues, with acidic residues surrounding the redox partner's functional group. Despite the relatively acidic character of cytochrome cc_3, the crevice of one heme is surrounded by a high number of positively charged residues, in the same manner as has been reported for cytochromes c_3. The environment of this heme is formed by four flexible surface loops which are variable in length and orientation in the different c_3-type cytochromes although the overall structural folds are very similar. It has been proposed that this region, adapted in topology and charge, is the interaction site for physiological partners and is also most likely to be the interaction site in the dimeric cytochrome cc_3.

Addresses: [1]Laboratoire de Cristallographie et Cristallisation des Macromolécules Biologiques, Institut de Biologie Structurale et Microbiologie, URA 1296, CNRS, 31 Chemin Joseph-Aiguier, 13402 Marseille cedex 20, France, [2]Laboratoire de Bioénergetique et Ingénierie des Protéines, Institut de Biologie Structurale et Microbiologie, UPR 9036, CNRS, 31 Chemin Joseph-Aiguier, 13402 Marseille cedex 20, France.

*Corresponding author.

Key words: cytochrome c_3, homodimer, molecular replacement, multiheme cytochrome, X-ray structure

Received: **7 Dec 95**
Revisions requested: **22 Dec 95**
Revisions received: **15 Jan 96**
Accepted: **19 Jan 96**

Structure 15 April 1996, **4**:395–404

Introduction

The octaheme cytochrome c_3 (M_r 26 000; hereafter referred to as cc_3) from *Desulfovibrio desulfuricans* Norway is one of several multiheme cytochromes characterized in sulfate-reducing bacteria. These bacteria are particularly rich in electron-transfer proteins, the exact roles of which have not yet been completely elucidated. The multiheme cytochromes are, in general, periplasmic and play a key role in the redox transfer chain between a periplasmic hydrogenase, which acts as the initial electron donor, and a complex membrane and cytoplasmic electron transfer chain, which uses oxidized sulfur compounds as terminal acceptors.

Three different c-type multiheme cytochromes have been identified and purified from *Desulfovibrio sp.*: the tetraheme cytochrome c_3 ([1–4]; hereafter referred to as c_3), which is uniformly present in all *Desulfovibrio sp.*, the octaheme cytochrome cc_3 [5,6] and a high molecular weight cytochrome (Hmc) containing 16 hemes [7–9]. These proteins all belong to class III of c-type cytochromes, as defined by Ambler [10]. On the basis of amino-acid-sequence alignment of these various cytochromes, it has recently been proposed that they form a cytochrome c_3 superfamily, together with a 3-heme-containing cytochrome from *Desulfuromonas acetoxidans* [11], and a common ancestral origin for the cytochromes of this superfamily has been postulated [12].

The occurrence of a soluble cytochrome Hmc (M_r 70000) has been reported in *Desulfovibrio vulgaris* strains Miyazaki and Hildenborough [7–8,13] and in *Desulfovibrio gigas* [9]. On the basis of sequence homology, this protein is considered to be a multidomain protein, with four c_3-like domains [8]. Furthermore, it could be a component of a transmembrane electron gate to the cytoplasm, as the Hmc

gene is the first open reading frame (*orf1*) of a 7kb operon containing five additional open reading frames (*orf2–6*) for transmembrane proteins [14].

Cytochrome cc_3 has only been isolated from *D. gigas* [6] and *D. desulfuricans* Norway [5]. The appearance of a 13 kDa apoprotein after SDS electrophoresis [15], as well as the nature of its electron paramagnetic resonance (EPR) spectra [16], indicated that this octaheme cytochrome is a homodimeric cytochrome c_3 with two identical subunits; it is different from the tetraheme cytochrome c_3 in its amino-acid composition and its EPR spectra. As in all c_3-type cytochromes, the four heme groups in each subunit display four distinct midpoint redox potentials, that is, four identical pairs because of the symmetry of the dimer. For the cytochrome cc_3 described here, the values, measured by cyclic voltametry, are –210, –270, –325 and –365mV, respectively [5].

The exact function and location of this protein have not yet been established. It has been shown that the homodimeric cytochrome cc_3 of *D. gigas* is able to stimulate sulfate reduction in a crude extract [17] and that it mediates the electron transfer between purified hydrogenase and sulfate reductase; cytochrome c_3 is almost inactive in the same reaction [18]. But this reaction might not be physiological as cytochrome cc_3 is supposed to be periplasmic and the sulfate reductase is cytoplasmic [19]. The second order homogeneous rate constant of the electron transfer between Ni–Fe–Se-hydrogenase and cytochrome cc_3 (reduction of cytochrome cc_3 by hydrogenase), which were purified from the same organism (*D. desulfuricans* Norway), was measured by cyclic voltametry [20] and yielded a value of 8×10^8 $M^{-1}s^{-1}$ in 100mM Tris-HCL pH 7.6. This compares advantageously to the value of 6×10^7 $M^{-1}s^{-1}$ obtained for the second order homogeneous rate constant of the reduction of cytochrome c_3 by the periplasmic hydrogenase, in the same medium. This rate constant showed a marked dependence on the ionic strength, which can be explained by repulsive forces between the redox partners. This is in view of the very acidic nature of both cytochrome cc_3, having an isoelectric point of 4.8, and hydrogenase (pI=6.0) [21]. A protein–protein electrostatic recognition process would necessitate either very localized charges at the interacting sites or an important role for intermediate ions.

The three-dimensional (3D) structures of several cytochromes c_3 from various species have been reported and compared [22–28]. The crystallization of homodimeric cytochromes cc_3 from *D. gigas* and *D. desulfuricans* Norway has been successful [29,30], but no 3D structure has been reported up to now. We describe, herein, the structure of cytochrome cc_3 from *D. desulfuricans* Norway, determined at 2.16 Å resolution. A preliminary structural analysis has been reported earlier [27].

Results and discussion

The architecture of the cytochrome cc_3 subunit

The crystal structure of cytochrome cc_3 has been determined by the molecular replacement method and has been refined against diffraction data to 2.16 Å resolution (Table 1). The asymmetric unit contains a monomeric subunit, the dimer being generated by a crystallographic twofold axis. The dimensions of the homodimeric cytochrome are $39\times70\times30$ $Å^3$, the longest dimension corresponding to the value measured across the dimer (Fig. 1). Besides 110 residues and the four heme groups, 65 water molecules and a sulfate ion have been modeled for each subunit, in order to account for the electron density in the ($2F_o–F_c$) map (Fig. 2). The sequence alignment for different cytochromes c_3 is shown in Figure 3. The heme numbering scheme, adopted in the present structure description, corresponds to the order of appearance in the primary sequence of the cysteines that covalently link the heme groups.

Table 1

Crystallographic data and model refinement.

	cc_3 at 20°C, crystals grown with ethanol		cc_3 at 4°C, crystals grown with $(NH_4)_2SO_4$+2%PEG 400	
Space group	$P3_121$		$P3_121$	
Cell dimensions (Å)	a=b=73.01 c=61.81		a=b=73.71 c=57.25	
Resolution range (Å)	28.0–2.14		27.8–2.16	
Total no. of observations	51 309		28 293	
No. of unique observations	10 359		9198	
% of data/R_{sym}*	93.0/6.5		92.4/8.9	
No. of non hydrogen atoms	1034		1034	
No. of solvent sites	71		65	
Ions modeled	–		1 SO_4^{2-}	
Missing residues	Glu1		Glu1	
	No cutoff	**>2σ**	**No cutoff**	**>2σ**
Resolution range (Å)	9.5–2.20	5.5–2.20	12–2.16	12–2.16
R factor (%)	23.0	20.9	20.4	14.7
No. of reflections	9837	8097	8455	4824
Free R factor (%)	31.0	27.0	26.3	20.7
No. of reflections	1017	811	897	507
Rms deviation in:				
Bond lengths (Å)	0.009		0.009	
Bond angles (°)	1.81		1.79	
Ramachandran outliers	none		none	

*$R_{sym} = \sum|I-\langle I\rangle|/\sum I$ where I=observed intensity and $\langle I\rangle$ = average intensity obtained from multiple observations of symmetry related reflections.

The monomeric subunit adopts the cytochrome c_3 fold [31], which has a significant number of secondary structure features (~25% helix, ~5% β sheet and ~20% β turns and 50% coil and loops [26]). The comparison of the sequences as well as the structural superposition of the different cytochromes having the cytochrome c_3 fold (Fig. 4 and Table 2), reveals that there are five regions that differ strongly from one cytochrome to the other, not only in their amino-acid composition but also in their

Figure 1

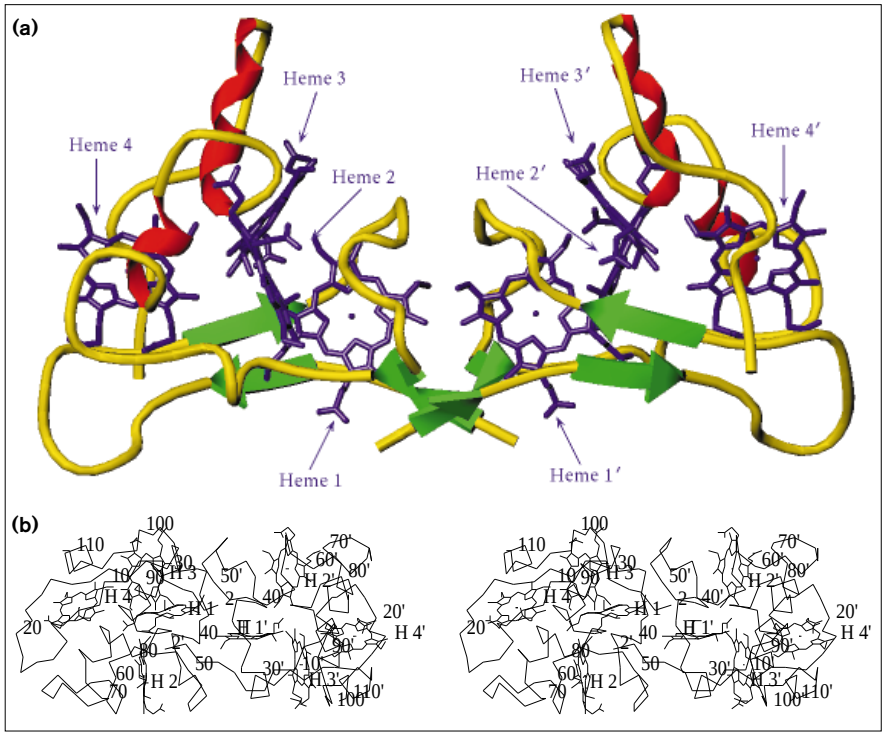

The overall structural fold of one subunit of the symmetrical dimeric cytochrome cc_3 from *D. desulfuricans* Norway is a c_3-type fold. **(a)** Ribbon representation of the Cα traces and the heme groups of the dimer. The crystallographic twofold axis lies in the plane of the representation. β strands are shown as green arrows and the α helices as red spirals. (Figure generated using TURBO-FRODO [53].) The orientation of the subunit on the right-hand side corresponds to that used for Figure 4. **(b)** Stereo diagram showing Cα traces and heme groups of the dimer. Hemes 1 to 4 and 1′ to 4′ are numbered H1 to H4 and H1′ to H4′. The orientation is perpendicular to that in (a).

structural arrangement. These five regions coincide with the regions defined as loops 1 to 5 by Higuchi *et al.* [31]. Apart from the five loops, large variations are only observed in the C-terminal and N-terminal regions.

Cytochrome cc_3 contains one short β sheet, formed by two antiparallel strands from residues 8–11 and 29–26, found at the same position in all cytochromes c_3. The length of loop 1, formed by the residues connecting the sequences of the β strands, varies strongly from one cytochrome c_3 to the other. In cytochrome c_3 from *D. vulgaris* Miyazaki and Hildenborough this loop is made up of six residues only; in cytochrome c_3 from *D. desulfuricans* Norway it contains 21 residues and in cytochrome cc_3 this loop has an intermediate length of 14 residues (see Fig. 3). The only extended α helix that is conserved in this kind of folding is formed by residues 71–96, situated between the binding sites of hemes 3 and 4. As in most cytochromes c_3 it is interrupted just behind residue His77 (the sixth axial ligand of the iron of heme 4) and a loop of six residues (loop 4) is inserted before continuing with the binding site of heme 3 at Cys86. Only in cytochrome c_3 from *D. desulfuricans* Norway is the helix uninterrupted, but is bent by 23° at the equivalent position [26]. Three other helical regions comprise the heme-binding sites of hemes 1 (Cys38 to His42) and 4 (Cys105 to His109) and a loop region (Val45 to Tyr49, within loop 2) situated at the interface of the dimer. Each of these three helices contains only five residues and forms one complete helical turn.

The subunit interactions of the dimer

The crystallographic twofold axis relates the two subunits of cytochrome cc_3 in such a way that hemes 1 of each subunit come to lie closest to each other. One of the two surface-exposed heme edges, the edge comprising pyrrole rings A and B (notation of the Protein Data Bank [32]),

Figure 2

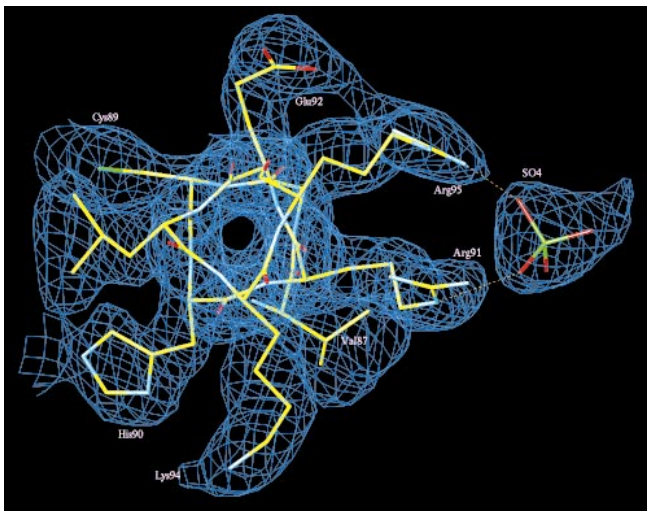

Quality of the electron-density map in the region of the sulfate ion. The final ($2F_o$–F_c) map at 2.16 Å is contoured at 1σ.

Figure 3

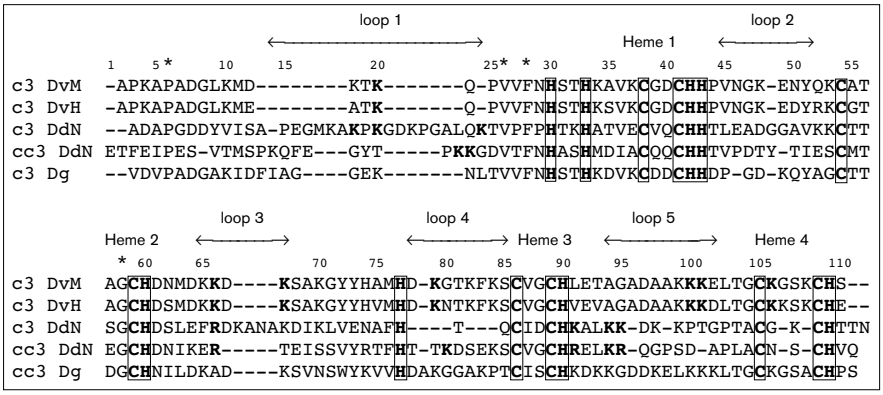

The sequence alignment based on the three-dimensional structures of the cytochromes c_3 from *D. vulgaris* Miyazaki (DvM), c_3 from *D. vulgaris* Hildenborough (DvH), c_3 from *D. desulfuricans* Norway (DdN), cc_3 from *D. desulfuricans* Norway (DdN) and c_3 from *D. gigas* (Dg). The indicated numbering scheme corresponds to the sequence of cytochrome cc_3 from *D. desulfuricans* Norway. The histidine residues directly following the second cysteine residue of the heme-binding sites are considered as the fifth axial ligands of the iron of the corresponding heme. The strictly conserved residues involved in the heme-binding sites are marked by the boxes. Four other strictly conserved residues are marked with an asterisk. The highlighted lysine and arginine residues are supposed to be involved in docking with physiological partners.

becomes buried in the dimer interface and the accessible surface area of heme 1 is diminished from 126 Å^2 to 62 Å^2. The iron atoms of hemes 1 and 1′ are at a distance of 15.1 Å, the shortest distance between the heme edges is 5.0 Å for the methyl groups of pyrrole rings B. A striking feature is a rather close contact between the cysteines 38 and 38′, which are covalently linked to the vinyl groups of pyrrole rings B of hemes 1 and 1′, respectively. The distance across the binding interface separating the sulfur atoms of these cysteines is 3.8±0.2 Å (mean coordinate error, derived from a Luzzati-plot). This is a little longer than the sum of the van der Waals radii of the two sulfur atoms (3.70 Å), but this close contact is nonetheless likely to be important for a possible electron pathway between the two subunits.

Figure 4

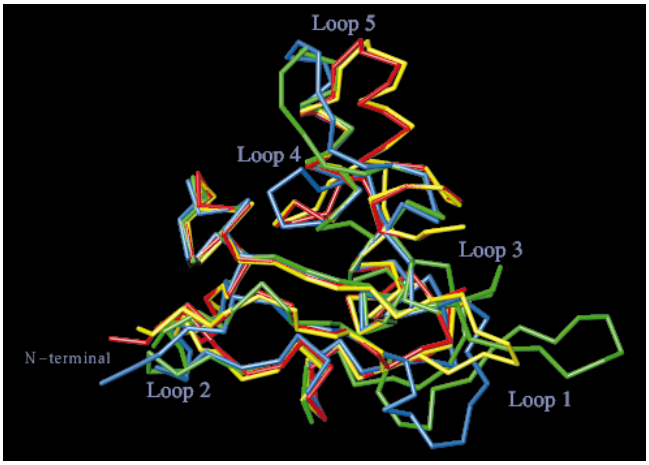

Superposition of the Cα traces of different cytochromes c_3 (see also Table 2). Cytochrome c_3 from *D. vulgaris* Miyazaki is coloured in red, cytochrome c_3 from *D. gigas* is in yellow, cytochrome c_3 from *D. desulfuricans* Norway is in green and a subunit of cytochrome cc_3 from *D. desulfuricans* Norway is coloured in blue. The five surface loops, as defined by Higuchi *et al.* [31], are shown.

The surface area becoming buried on each subunit on formation of the dimer is about 913 Å^2, which is 6% of the total accessible surface area for cytochrome cc_3. This value compares well to interface surface areas in the range of 600 to 1600 Å^2, reported to be typical for protein–protein interaction complexes or oligomers [33]. In all, 15 residues of each subunit, distributed in three major regions of cytochrome cc_3, are implicated in the formation of the dimer: the N-terminal residues 2–5, residues 36–39 of heme-binding site 1 and residues 49–51 of loop 2. Furthermore, close contacts within the interface are also found for residues 7, 31, 34 and 46 and the propionate group of heme 1. The average main- and side-chain B factors for the 15 residues situated at the interface are 22.6 Å^2 and 25.3 Å^2, respectively, compared with the respective values of 28.3 Å^2 and 30.9 Å^2 for all residues (the heme groups are not included). No salt bridge is formed between the two subunits. Besides the eight hydrogen bonds formed across the interface (Table 3), only van der Waals contacts between hydrophobic residues exist on the interface. For example, the aromatic side chains of residues Phe3 and Phe3′, related by the twofold crystallographic axis, participate in hydrophobic stacking (the average C–C′ distance is 3.6 Å). 53% of the interface can be considered as non polar, 33% as polar and 14% as charged, the charged residues all being situated on the periphery of the interface. Residues 3–5 form a short antiparallel β sheet with residues 51′–49′ of the symmetrical subunit, which is duplicated by the twofold axis. The interface can therefore be described as a combination of loop interactions and extended β sheets, motifs which are typical for dimer interfaces as defined by Miller [34].

Sequence comparison (Fig. 3) shows that in the segments implicated in the formation of the dimer interface a number of amino-acid-substitutions occur in cytochrome cc_3 with respect to cytochromes c_3. These completely change the nature or size of the amino acid: Phe3 of cytochrome cc_3 substitutes smaller, non-aromatic residues; Glu7 substitutes

Table 2

Structural similarity of cytochrome cc_3 from *D. desulfuricans* Norway with cytochromes c_3.

Cytochromes compared	No. of residues	Rmsd of 4 Fe atoms (Å)	No. of Cα atoms	Rmsd* (2 Å)	No. of Cα atoms	Rmsd* (1 Å)
c_3DdN†–cc_3DdN‡	118–110	0.43	82	1.01	54	0.62
c_3Dg§–cc_3DdN	112–110	0.43	71	1.02	42	0.60
c_3DvM–cc_3DdN	107–110	0.31	68	0.88	51	0.53
c_3DdN–c_3DvM#	118–107	0.56	75	1.04	44	0.63
c_3DdN–c_3Dg	118–112	0.69	75	1.04	47	0.66
c_3DvM–c_3Dg	107–112	0.28	100	0.72	84	0.54

*Superposition of Cα positions was achieved by rigid-body refinement in two steps permitting maximal deviations between corresponding atoms of 2 Å at first and 1 Å in a second step.
†c_3DdN, cytochrome c_3 (M_r 13 000) from *D. desulfuricans* Norway;
‡cc_3DdN, cytochrome c_3 (M_r 26 000) from *D. desulfuricans* Norway;
§c_3Dg, cytochrome c_3 (M_r 13 000) from *D. gigas*;
#c_3DvM, cytochrome c_3 (M_r 13 000) from *D. vulgaris* Miyazaki.

small hydrophobic residues; Ala31 substitutes bulkier, hydrophilic residues, Gln39 replaces glycine, valine or aspartic acid; Tyr49 is inserted in loop 2. These particular substitutions all involve tightly bound residues within the interface in cytochrome cc_3 and seem to be responsible for the formation of the dimer. The structural results therefore support the findings, that this cytochrome is a physiological dimer [5] and not just the result of a polymerization during the purification procedures, reported to be frequent for this type of protein [15].

The heme environments

As in all other cytochromes c_3, the fifth and sixth axial ligands of the heme iron atoms in cytochrome cc_3 are histidines, resulting in particularly low redox potentials. The geometry of the heme ligation and the relative orientations of the histidine planes with respect to the heme planes have been described elsewhere [27]. The relative His-plane angles and the residues hydrogen bonded to the Nδ1 of the histidines (axial ligands of the heme iron atoms) show stronger similarity to those in cytochromes c_3 from *D. vulgaris* Miyazaki, Hildenborough and *D. gigas* than to those in cytochrome c_3 from *D. desulfuricans* Norway. As in cytochromes c_3 from *D. vulgaris* Miyazaki, Hildenborough and *D. gigas* a tyrosine (Tyr73) is found parallel to His77 (the sixth axial ligand of heme 4) and the relative His-plane angles of hemes 3 and 4 are closer to the parallel orientation, 12° for the His-planes around heme 3 and 0.2° around heme 4. This should be compared with 25.6° and 77.2° for the respective His-plane angles found in the tetraheme cytochrome c_3 from *D. desulfuricans* Norway. Interestingly, a strictly conserved water molecule, forming a hydrogen bond to Nδ1 of the histidine, the fifth axial ligand of heme 1, has been observed in all cytochrome c_3 structures [23,25–28]; it is also present in both models obtained from the two different crystallization conditions for cytochrome cc_3 from *D. desulfuricans* Norway (Fig. 5). This tightly bound water molecule, buried in the pocket of heme 1, is likely to play an important role in the electron-transfer mechanism, as has been proposed by Matias *et al.* [25].

Table 3

Hydrogen bonds and close contacts on the interface of the dimer.

Atom on subunit A	Atom on subunit A′	Hydrogen-bond distance (Å)
Thr2-N	Ile51-O	3.1
Thr2-N	Hem1-O2A	2.8
Phe3-O	Ile51-N	3.0
Ile5	Tyr49-O	2.9
Glu7-OE2	Tyr49-OH	3.0
Met34-O	Gln39-NE2	3.0
Ile36-O	Gln39-NE2	2.8
Cys38-N	Gln39-OE1	3.2
		Close contacts
Cys38-SG	Cys38-SG	3.8
Phe3-CG	Phe3-CD1	3.3
Phe3-CD1	Phe3-CD1	3.4
Phe3-CD2	Phe3-CZ	3.3
Phe3-CE2	Phe3-CE2	3.3

As mentioned above, cytochrome cc_3, in contrast to c_3, from *D. desulfuricans* Norway has the same loop insertion in the α helix between hemes 3 and 4 as found in cytochromes c_3 from *D. vulgaris* Miyazaki, Hildenborough and *D. gigas*. This loop covers up one of the heme edges of heme 2, which is highly exposed to the solvent region in cytochrome c_3 from *D. desulfuricans* Norway [26].

The relative orientations of the heme porphyrin rings with respect to the polypeptide chain is to a high degree comparable with the arrangement observed in all other cytochromes c_3. In this arrangement, the edges exposed to the solvent region in hemes 1 and 4 are composed of pyrrole rings A and B, reported as typical for cytochrome c-type hemes [35]; for hemes 2 and 3, pyrrole rings C and D are exposed. The difference in this cytochrome c_3 is that the pyrrole ring B of heme 1 is buried in the interface of the dimer. Solvent exposed atoms for the four heme

Figure 5

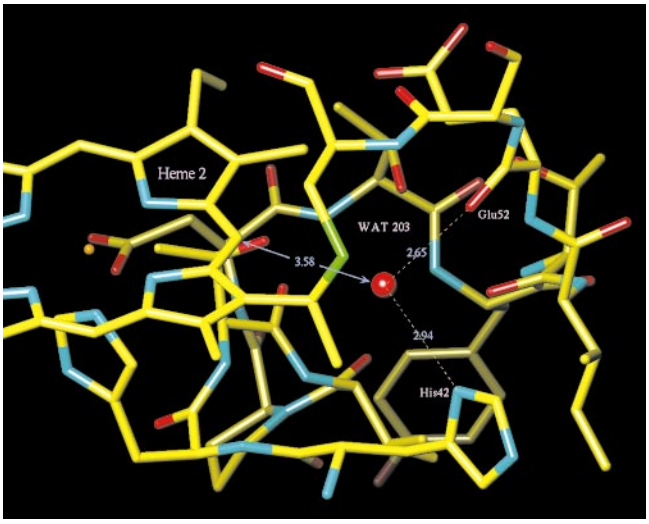

The strictly conserved water molecule found in the heme pocket of heme 1 for all cytochromes c_3 for which the 3D structures have been determined. In cytochrome cc_3 from *D. desulfuricans* Norway it forms a hydrogen bond to Nδ1 of His42, the fifth axial ligand of heme 1, and the main-chain carboxyl oxygen of Glu52. The water molecule is also rather close to one edge of heme 2.

Table 4

Solvent exposure of the heme edges.

	Cysteine atom	Surface (Å^2)	Heme atom	Surface (Å^2)
Heme 1			CMA	3
			CGA	10
			O1A	17
			O2A	7
			O1D	10
Heme 2			CBA	7
			CGA	12
			O1A	3
			O2A	27
	Cys59 SG	1	CAC	2
			CBC	23
			CMD	47
			CBD	40
			CGD	14
			O1D	22
			O2D	19
Heme 3			CMA	6
			CBA	29
			CGA	8
			O1A	1
			O2A	13
	Cys89 SG	1	CBC	10
			CMD	28
			CGD	17
			O1D	9
			O2D	33
Heme 4			CMA	12
	Cys105 CB	7	CMB	31
	Cys105 SG	21	CBB	51

groups are listed in Table 4. It is worthwhile mentioning that in all other cytochromes c_3, for both hemes 1 and 4, one cysteine residue, covalently linked to the vinyl group of the pyrrole ring B, is highly exposed to the solvent region, whereas all other cysteines are relatively buried by the polypeptide chain [23,26]. The exposure of thioether linkages has repeatedly been proposed to play an important role in interactions with other macromolecules [36,23], that is, the physiological redox partners. In this cytochrome cc_3, only one thioether linkage is exposed to solvent, namely Cys105 which is linked to pyrrole ring B of heme 4, as the second thioether linkage is buried in the interface of the dimer. This observation supports the often discussed assumption that heme 4 is the site of interaction between cytochromes c_3 and its physiological partners within the electron pathway of sulfate-reducing bacteria [37].

Heme 4, the assumed interaction site for physiological redox partners

The question concerning the role of the four (or eight) hemes present in this cytochrome family has been investigated using various techniques, such as molecular modeling, NMR, EPR, kinetic and microcalorimetric studies, but the issue remains unresolved for three of the four hemes. There is some information concerning the role of heme 4; all data available indicate that it is most likely to be the interaction site between cytochromes c_3 and their physiological partners [25,37–43]. The construction of a hypothetical complex between cytochrome c_3 from *D. desulfuricans* Norway and ferredoxin I [38] showed that the most appropriate interaction would involve heme 4; peptide mapping of the covalent cytochrome c_3–ferredoxin I complex confirmed this model [40,43]; molecular modeling together with NMR studies of a rubredoxin–cytochrome c_3 complex also indicated that heme 4 was the interaction site [39]. The analysis of the thermodynamic parameters dependent on the ionic strength revealed a considerable electrostatic effect on the cytochrome c_3–ferredoxin complex formation [44]. This is consistent with the idea that the interaction of this type of cytochrome is based on a heme crevice surrounded by positively charged lysine residues. The crevice is a feature common to all c_3-type cytochromes and would interact with acidic residues surrounding the redox partner's functionally active group [37–44]. However, no studies concerning possible interactions of this type for cytochrome cc_3 have been reported up to date.

The superposition of the interaction sites (the heme 4 crevice) of the different cytochromes c_3 with the crevice of heme 4 of one subunit of cytochrome cc_3 is illustrated in Figure 6. A striking feature is that the environment of heme 4 is formed by four of the five loop regions, namely loops 1, 3, 4 and 5, which differ strongly from one

Figure 6

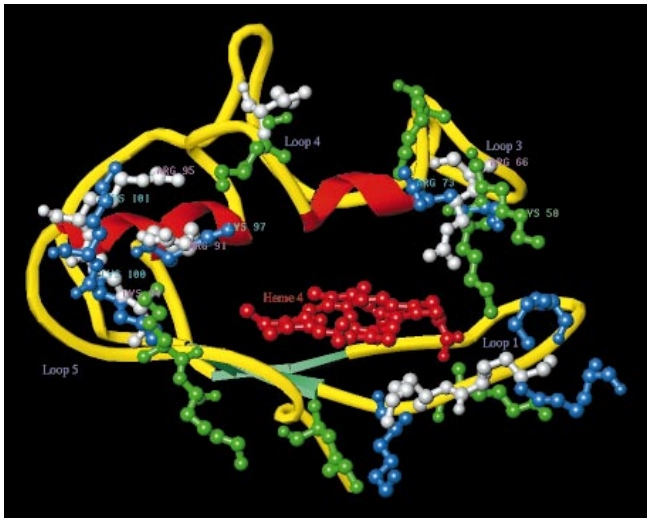

A ribbon representation of cytochrome cc_3. The lysine and arginine residues surrounding the crevice of heme 4 (red), are shown with their relative position and orientation for cytochrome c_3 from *D. vulgaris* Miyazaki (green), cytochrome cc_3 from *D. desulfuricans* Norway (white) and cytochrome c_3 from *D. desulfuricans* Norway (blue).

cytochrome c_3 to the other (see also Fig. 3). In all structure determinations these loops have been reported to show high B-factor values and most residues within these same loop regions show poorly defined electron density [22–27]. These findings seem to point to the loop-regions 1–5 not only displaying high variations when comparing one cytochrome c_3 structure with another, but also suggest they are disordered and/or very flexible in each cytochrome c_3. One can also see that the lysine and arginine residues, which have been proposed to be involved in complex formation [37–39], occur within these loop regions (highlighted in the sequence alignment, Fig. 3). In particular, 7 of the 11 lysine and arginine residues present in cytochrome cc_3 are situated in the close environment of heme 4 (Table 5). Despite the overall acidic character of cytochrome cc_3 (pI 4.8; 16 negatively charged residues against 11 positively charged residues), there are only few negatively charged residues in the region around heme 4 and the local net charge will be positive. The structural superposition of the different cytochromes c_3 makes clear that although all the highly conserved lysines in the cytochrome c_3 family are localized in the same regions with respect to the heme 4 crevice, the structural superposition is rarely observed (Table 5 and Fig. 6). One residue, Arg66, superposes at the Cα position with a lysine in cytochromes c_3 from *D. vulgaris* Miyazaki and Hildenborough and *D. desulfuricans* Norway, and three residues, namely Arg91, Lys94 and Lys95, are well aligned with lysines in cytochrome c_3 from *D. desulfuricans* Norway. This fact is not surprising as the monomeric cytochrome c_3 and the dimeric cytochrome cc_3, present in *D. desulfuricans* Norway are supposed to interact with different physiological partners. The flexibility of the four loops, surrounding the crevice of heme 4, and the slightly different locations of the positively charged residues modulates their specificity and their mode of interaction with the different physiological partners.

A recent study of the interfacial behaviour of the polyheme cytochromes, using the monomolecular film technic, in order to determine whether and how these cytochromes interact with (phospho-) lipids [45], has shown that differences are measurable in the penetration capacity of the various cytochromes c_3 into lipid layers bearing different charges. The *D. vulgaris* Hildenborough cytochrome hmc, containing 16 hemes, and *D. desulfuricans* Norway tetra- and octaheme cytochromes c_3, which have been assumed to be soluble periplasmic proteins, may be considered as extrinsic membrane proteins, unlike the *D. vulgaris* Hildenborough cytochrome c_3. It has been proposed that the association with the outer face of the cytoplasmic membrane would implicate the amphiphilic loop 1 (Ala12–Leu28) near heme 4 in cytochrome c_3 and the corresponding region in cytochrome cc_3 [45]. Consequently, this loop may have functional relevance in the interaction with the membrane and these cytochromes may constitute the missing link between periplasm and membrane.

In general, these results seem to indicate that the cytochromes c_3 have a common interaction site for different physiological partners: the crevice of heme 4, which is

Table 5

Charged residues surrounding the crevice of heme 4 in different cytochromes c_3 and corresponding residues in cytochrome cc_3 as deduced by structural superposition.

c_3 DvH/M*			K15				K57	K58	K60	K72				K94	K95	K101
Surface exposure (Å²)			191				95	166	113	155				94	105	163
c_3 DdN†	K19	K21				K30		R73			K97	K100	K101			
Surface exposure (Å²)	108	131				89		105			146	99	182			
cc_3 DdN				K22	K23			R66		K80	R91	K94	R95			
Surface exposure (Å²)				143	53			137		171	87	78	147			

Residues which superpose structurally at the Cα position appear in the same column (see also Fig. 6). *DvH/M, *Desulfovibrio vulgaris* Hildenborough/Miyazaki; †DdN, *Desulfovibrio desulfuricans* Norway.

conserved during evolutionary events of the multiheme cytochromes. The modulation of the specificity of interaction is assured by different topological setups, such as the variation of length and flexibility of surface loops. These are adaptable to the complementary surface of the partner, and to the difference in the distribution of the charged residues within these regions.

Biological implications

Sulfate-reducing bacteria are strict anaerobes that derive energy for metabolic processes from sulfate respiration. The electron-transport chain in *Desulfovibrio* species, which links the periplasmic oxidation of hydrogen to the cytoplasmic reduction of sulfate, is unusual in that it involves a number of periplasmic multiheme cytochromes *c*. The soluble octaheme cytochrome c_3 (M_r 26000) could play an important role as an electron carrier between the periplasmic hydrogenase and membrane bound electron transfer proteins.

Following the discovery of an increasing number of cytochromes *c* in sulfate and sulfur-reducing bacteria, the existence of a cytochrome c_3 superfamily has been described. This includes various multiheme cytochromes all belonging to the class III of cytochromes *c* described by Ambler [10]. Three dimensional (3D) structures are presently available only for tetraheme cytochromes c_3 (M_r 13000). The structure of *D. desulfuricans* Norway octaheme cytochrome c_3 (M_r 26000) is the first described for this type of cytochrome.

The knowledge and the comparison of the 3D structures of these polyhemic cytochromes provides a structural basis for understanding the factors controlling the redox potential and therefore the intra- and intermolecular electron transfer. The 3D structures are also important in elucidating the interaction processes whereby the domains are recognized by specific redox partners or are implicated in possible membrane association.

The structural aspect of electron transfer within protein complexes is an important point of current research. Two parameters are driving forces in electron exchange within a complex, namely the interacting domain and the electron pathway. Multiheme cytochromes are an interesting superfamily for which kinetic parameters and X-ray structures have been extensively studied in view of these factors. There is evidence for an intramolecular electron flow and protein engineering has now been developed to elucidate the functional role of this electron exchange. Structural comparison of different cytochromes c_3 supports the assumption that one of the hemes is the site of interaction between the molecule and diverse redox partners. The reasons for the presence of the other prosthetic groups and for the intramolecular electron exchange still need to be determined. The knowledge of the 3D structure of a new compound of the cytochrome c_3 superfamily provides an opportunity to consider the structural and functional aspects of this molecule in comparison with the previous data obtained on monomeric cytochromes c_3.

On the basis of amino-acid-sequence alignments of these various cytochromes, a common ancestral origin may be postulated for the cytochrome c_3 family. Determining the 3D structure of other members of this family could help in understanding the mechanism involved in the folding and evolution of the polyheme cytochromes. The role of the various cytochromes and the compartmentation of the redox processes in which they are involved, between the periplasm and the cytoplasm, as well as the nature of the membrane redox proteins associated, are presently under study.

Materials and methods

Data collection

The crystal, which was used for the data collection at 20°C, was grown under the same conditions as described elsewhere [30]. The space group is trigonal $P3_121$ with cell dimensions a=b=73.01 Å, c=61.81 Å and one monomeric subunit of the cytochrome cc_3 in the asymmetric unit. This leads to a value V_m=3.2 Å^3 Da^{-1} and a solvent content of about 60%, which compares to experimentally observed values reported for protein crystals in general [46]. The second crystal, which led to the data set at 4°C, was grown by vapor diffusion in hanging drops [47], at pH 7.6 (0.1M Hepes), with a 2M solution of $(NH_4)_2SO_4$ and 2% polyethylene glycol (PEG) 400 as precipitating agent. These crystals belonged to the same space group but had different cell parameters (a=b=73.71 Å, c=57.25 Å). The overall crystal packing did not change from one crystal to the other and the solvent content is almost the same (60 and 59%, respectively).

All data were measured with conventional Cu-Ka X-radiation by means of a Rigaku RU-200 rotating anode operating at 40kV, 80mA with a graphite monochromator. Data were collected on a MAR-research imaging plate detector at room temperature (20°C) in the case of the first crystal and at controlled temperature (4°C) for the second crystal. The first data set, collected at 20°C, was integrated with MOSFLM [48] and the second with XDS [49]. Further processing was carried out using the CCP4 package [50].

Molecular replacement and structure refinement

The structure of the dimeric cytochrome cc_3 was solved by performing molecular replacement with the program AMoRe [51]. At first a truncated (poly-Ala) search model was constructed on the basis of the refined structure of cytochrome c_3 [26] from the same *Desulfovibrio* species (the two cytochromes display 34.6% homology on the basis of sequence alignment). On the basis of the first data set, collected at 20°C, two equivalent solutions related by a twofold symmetry were found, indicating that the asymmetric unit contains one monomeric subunit. The dimer is generated by the crystallographic twofold axis. After rigid-body refinement, the preliminary calculated R factor was 48.5% and a first energy minimization with XPLOR 3.1 [52] lowered the R factor to a value of 37.2%. At this stage, solvent-flattened (F_o-F_c) and ($2F_o$-F_c) maps were calculated to permit model construction with the graphical display package TURBO-FRODO [53]. A full model, based on the sequence information for cytochrome cc_3 [11], could be placed into the electron-density map. Several simulated annealing refinement cycles were performed with XPLOR 3.1 and 100 water molecules were fitted. The

R factor converged to a value of 20%; the Ramachandran plot [54] of the structure showed that the model had reasonable stereochemistry; however, no supplementary information could be deduced from either solvent-flattened or omit-maps, calculated at this stage of refinement, in order to optimize the model and lower the R factor. In fact, the model had a very high average temperature factor of 47.1 Å^2 and two surface loops, containing residues 14–23 and 63–69, were poorly defined in the electron-density maps. Assuming that some structural disorder and/or dynamical flexibility of parts of the protein led to this final stage of refinement, with elevated R factor and temperature factor, we collected a second data set at controlled temperature of 4°C. Again, the model was positioned with respect to this new data set by performance of the molecular replacement method. The same solutions were found, mainly translated along the c-axis, as to be expected with respect to the changes in the cell parameters. After several refinement cycles, the final atomic model shows only small differences (0.43 Å rms deviation of the 110 Cα atoms) from the model calculated from the data set at 20° C (Table 1). The electron density for the surface loops 14–23 and 63–69 still showed interruptions but the overall aspect of the map was better. The average temperature factor for this model was 26.1 Å^2. 110 out of the 111 residues could be modeled, but no density was visable for the first residue (Glu1). 65 water molecules were placed and a sulfate ion was located close to two arginine residues (Arg91 and Arg95; Fig. 2). 88% of the residues are in the most favoured regions of the Ramachandran plot.

The atomic coordinates of the refined structural model have been deposited with the Brookhaven Protein Data Bank (PDB ID: 1CZJ).

The determination of the rms deviations and the comparison of the different c_3-type cytochromes was accomplished by the superposition of the Cα backbone traces and the heme groups, with the option for rigid-body refinement, using the graphics program TURBO-FRODO [53]. After a visual superposition on the basis of the heme group arrangement, a first step of rigid-body refinement was performed considering only atoms closer than a 2 Å cutoff and, in a second step, all atoms closer than 1 Å (Table 2).

Acknowledgements

We would like to thank Pedro M Matias at the ITQB, Lisbon, Portugal, for giving us the coordinates of the three-dimensional model of cytochrome c_3 from *D. gigas*, not yet available from the Protein Data Bank. We gratefully acknowledge the Fermentation Unit (IBSM-LCB, CNRS, Marseille, France) for growing the bacteria.

References

1. Yagi, T. & Maruyama, K. (1971). Purification and properties of cytochrome c_3 of *Desulfovibrio vulgaris* (Miyazaki). *Biochim. Biophys. Acta* **243**, 214–224.
2. Biebl, H. & Pfennig, N. (1977). Growth of sulfate-reducing bacteria with sulfur as electron acceptor. *Arch. Microbiol.* **112**, 115–117.
3. Le Gall, J. & Forget, N. (1978). Purification of electron transfer components from sulfate-reducing bacteria. *Methods Enzymol.* **53**, 613–633.
4. Bruschi, M. (1981). The primary structure of the tetraheme cytochrome c_3 from *Desulfovibrio desulfuricans* (Strain Norway 4). *Biochim. Biophys. Acta* **671**, 219–226.
5. Loutfi, M., Guerlesquin, F., Bianco, P., Haladjian, J. & Bruschi, M. (1989). Comparative studies of polyhemic cytochromes *c* isolated from *Desulfovibrio vulgaris* (Hildenborough) and *Desulfovibrio desulfuricans* (Norway). *Biochem. Biophys. Res. Commun.* **159**, 670–676.
6. Bruschi, M., Le Gall, J., Hatchikian, E.C. & Dubourdieu, M. (1969). Cristallisation et propriétés d'un cytochrome intervenant dans la réduction du thiosulfate par *Desulfovibrio gigas*. *Bull. Soc. Fr. Physiol. Veg.* **15**, 381–390.
7. Pollock, W.B.R., *et al.*, & Voordouw, G. (1991). Cloning, sequencing and expression of the gene encoding the high molecular weight cytochrome c_3 from *Desulfovibrio vulgaris* Hildenborough. *J. Bacteriol.* **173**, 220–228.
8. Bruschi, M., *et al.*, & Voordouw, G. (1992). Biochemical and spectroscopic characterization of the high molecular weight cytochrome *c* from *Desulfovibrio vulgaris* Hildenborough expressed in *Desulfovibrio desulfuricans* G200. *Biochemistry* **31**, 3281–3288.
9. Chen, L., Pereira, M.M., Teixeira, M., Xavier, A.V. & Le Gall, J. (1994). Isolation and characterization of a high molecular weight cytochrome from the sulfate reducing bacterium *Desulfovibrio gigas*. *FEBS lett.* **347**, 295–299.
10. Ambler, R.P. (1991). Sequence variability in bacterial cytochromes *c*. *Biochim. biophys. Acta* **1058**, 42–47.
11. Bruschi, M., Leroy, G., Guerlesquin, F. & Bonicel, J.(1994). Amino-acid sequence of the cytochrome c_3 (M_r 26000) from *Desulfovibrio desulfuricans* Norway and a comparison with those of the other polyhemic cytochromes from *Desulfovibrio*. *Biochem. Biophys. Acta.* **1205**, 123–131.
12. Bruschi, M. (1994). Cytochrome c_3 (M_r 26000) isolated from sulfate-reducing bacteria and its relationships to other polyhemic cytochromes from *Desulfovibrio*. *Meth. Enzymol.* **243**, 140–155.
13. Higuchi, Y., Inaka, K., Yasuoka N. & Yagi, T. (1987). Isolation and crystallization of high molecular weight cytochrome from *Desulfovibrio vulgaris* Hildenborough. *Biochim. Biophys. Acta* **911**, 341–348.
14. Rossi, M., *et al.*, & Voordouw, G. (1993). The hmc operon of *Desulfovibrio vulgaris* subsp. Hildenborough encodes a potential transmembrane redox protein complex. *J. Bacteriol.* **175**, 4699–4711.
15. Guerlesquin, F., Bovier-Lapierre, G. & Bruschi, M. (1982). Purification and characterization of cytochrome c_3 (M_r 26000) isolated from *Desulfovibrio desulfuricans* Norway strain. *Biochem. Biophys. Res. Commun.* **106**, 530–538.
16. Le Gall, J., Bruschi-Heriaud, M. & Dervartanian, D.V. (1971). Electron paramagnetic resonance and light absorption studies on c-type cytochromes of the anaerobic sulfate reducer *Desulfovibrio*. *Biochim. Biophys. Acta* **234**, 499–522.
17. Hatchikian, E.C., Le Gall, J., Bruschi, M. & Dubourdieu, M. (1972). Regulation of the reduction of sulfite and thiosulfate by ferredoxin, flavodoxin and cytochrome cc_3 in extracts of the sulfate reducer *Desulfovibrio gigas*. *Biochim. Biophys. Acta* **258**, 701–708.
18. Bruschi, M., Hatchikian, E.C., Golovleva, L.A. & Le Gall, J. (1977). Purification and characterization of cytochrome c_3, ferredoxin and rubredoxin isolated from *Desulfovibrio desulfuricans* Norway. *J. Bacteriol.* **129**, 30–38.
19. Meyer, T.E. & Cusanovich, M.A. (1989). Structure, function and distribution of soluble bacterial redox proteins. *Biochim. Biophys. Acta.* **975**, 1–28.
20. Haladjian, J., Bianco, P., Guerlesquin, F. & Bruschi, M. (1991). Kinetic studies of the electron exchange reaction between the octaheme cytochrome c_3 (M_r 26000) and the hydrogenase from *Desulfovibrio desulfuricans* Norway. *Biochem. Biophys. Res. Commun.* **179**, 605–610.
21. Rieder, R. Cammack, R. & Hall, D.O. (1984). Purification and properties of the soluble hydrogenase from *Desulfovibrio* desulfuricans (strain Norway 4). *Eur. J. Biochem.* **145**, 637–643.
22. Haser, R., *et al.*, & Le Gall, J. (1979). Structure and sequence of the multihaem cytochrome c_3. *Nature* **282**, 806–810.
23. Higuchi, Y., Kusunoki, M., Matsuuna, Y., Yasuoka, N. & Kakudo, M. (1984). Refined structure of cytochrome c_3 at 1.8 Å resolution. *J.Mol.Biol.* **172**, 109–139.
24. Morimoto, Y., Tani, T., Okumura, H., Higuchi, H. & Yasuoka, N. (1991). Effects of amino acid substitution on the three-dimensional structure: an X-ray analysis of cytochrome c_3 from *Desulfovibrio vulgaris* Hildenborough at 2 Å resolution. *J. Biochem.* **110**, 532–540.
25. Matias, P.M., Frazao, C., Morais, J., Coll, M. & Carrondo, M.A. (1993). Structure analysis of cytochrome c_3 from *Desulfovibrio vulgaris* Hildenborough at 1.9 Å resolution. *J. Mol. Biol.* **234**, 680–699.
26. Czjzek, M., Payan, F., Guerlesquin, F., Bruschi, M. & Haser, R. (1994). Crystal structure of cytochrome c_3 from *Desulfovibrio desulfuricans* Norway at 1.7 Å resolution. *J. Mol. Biol.* **243**, 653–667.
27. Czjzek, M., Payan, F. & Haser, R. (1994). Molecular and structural basis of electron transfer in tetra- and octa-heme cytochromes. *Biochimie* **76**, 546–553.
28. Morais, J., *et al.*, & Carrondo, M.A. (1995). Structure of the tetraheme cytochrome from *Desulfovibrio desulfuricans* ATCC 27774: X-ray diffraction and Electron paramagnetic resonance studies. *Biochem*istry **34**, 12830–12841.
29. Sieker, L.C., Jensen, L.H. & Le Gall, J. (1986). Preliminary X-ray studies of the tetraheme cytochrome c_3 and the octaheme cytochrome c_3 from *Desulfovibrio gigas*. *FEBS Lett.* **209**, 261–264.
30. Czjzek, M., *et al.*, & Haser, R. (1992). Crystallization and preliminary crystallographic study of an octaheme cytochrome c_3 from *Desulfovibrio desulfuricans* Norway. *J. Mol. Biol.* **228**, 995–997.
31. Higuchi, Y., Kusunoki, M., Yasuoka, N., Kakudo, M. & Yagi, T. (1981). On cytochrome c_3 folding. *J. Biochem.* **90**, 1715–1723.

32. Bernstein, F. C., *et al*., & Tasumi, M. (1977). The Protein Data Bank: a computer-based archival file for macro-molecular structures. *J. Mol. Biol*. **112**, 535–542.
33. Janin, J. & Chothia, C. (1990). The structure of protein–protein recognition sites. *J. Biol. Chem*. **265**, 16027–16030.
34. Miller, S. (1989). The structure of interfaces between subunits of dimeric and tetrameric proteins. *Prot. Eng*. **3**, 77–83.
35. Stellwagen, E. (1978). Haem exposure as the determinate of oxidation-reduction potential of haem proteins. *Nature* **275**, 73–74.
36. Pelletier, H. & Kraut, J. (1992). Crystal structure of a complex between electron transfer partners, cytochrome c peroxidase and cytochrome c. *Science* **258**, 1748–1755.
37. Guerlesquin, F., Dolla, A. & Bruschi, M. (1994). Involvement of electrostatic interactions in cytochrome *c* complex formations. *Biochim*. **76**, 515–523.
38. Cambillau, C., Frey, M., Moss, J., Guerlesquin, F. & Bruschi, M. (1988). Model of a complex between the tetraheme cytochrome c_3 and the ferredoxin I from *Desulfovibrio desulfuricans* Norway strain. *Proteins* **4**, 63–70.
39. Stewart, D. E., *et al*., & Wampler, J. E. (1989). Electron transport in sulfate-reducing bacteria. Molecular modelling and NMR studies of the rubredoxin-tetraheme-cytochrome-c_3 complex. *Eur. J. Biochem*. **185**, 695–700.
40. Dolla, A. & Bruschi, M. (1988). The cytochrome c_3–ferredoxin electron transfer complex: cross-linking studies. *Biochim. Biophys. Acta.* **932**, 26–32.
41. Dolla, A., *et al*., & Gayda, J.P. (1989). Cytochrome c_3 - ferredoxin I covalent complex: evidence for an intramolecular electron exchange in cytochrome c_3. *Biochim. Biophys. Acta*. **975**, 395–398.
42. Dolla, A., Guerlesquin, F., Bruschi, M. & Haser, R. (1991). Ferredoxin electron transfer site on cytochrome c_3. Structural hypothesis of an intramolecular electron transfer pathway within a tetra-heme cytochrome. *J. Mol. Recogn*. **4**, 27–33.
43. Dolla, A., Leroy, G., Guerlesquin, F. & Bruschi, M. (1991). Identification of the site of interaction between cytochrome c_3 and ferredoxin using peptide mapping of the cross-linked complex. *Biochem. Biophys. Acta*. **1058**, 171–177.
44. Guerlesquin, F., Sari, J. C. & Bruschi, M. (1987). Thermodynamic parameters of cytochrome c_3-ferredoxin complex formation. *Biochemistry* **26**, 7438–7443.
45. Florens, L., *et al*., & Bruschi, M. (1995). Interfacial properties of the polyheme cytochrome c_3 superfamily from *Desulfovibrio*. *Biochemistry* **34**, 11327–11334.
46. Matthews, B. W. (1968). Solvent content of protein crystals. *J. Mol. Biol*. **33**, 491–497.
47. McPherson, A. (1982). *Preparation and Analysis of Protein Crystals*. pp. 96–97, Wiley and Sons, New York.
48. Leslie, A.G.W., Brick, P. & Wonacott, A.J. (1986). MOSFLM. *Daresbury Lab. Inf. Quart. Prot. Cryst.* **18**, 33–39.
49. Kabsch, W. (1988). Evaluation of single crystal X-ray diffraction data from a position-sensitive detector. *J. Appl. Cryst*. **21**, 916–924.
50. Collaborative computational project, No. 4. (1994). The CCP4 suite: programs for protein crystallography. *Acta Cryst*. D **50**, 760–763.
51. Navaza, J. (1994). AMoRe: an Automated Package for Molecular Replacement. *Acta Cryst.* A **50**, 157–163.
52. Brünger, A. T. (1993). *X-PLOR, Version 3.1*. Yale University, New Haven, CT.
53. Roussel, A. & Cambillau, C. (1992). *TURBO-FRODO, the manual*. Biographics, LCCMB, Marseille, France.
54. Ramachandran, G.N. & Sasisekharan, V. (1968). Conformation of polypeptides and proteins. *Adv. Protein Chem*. **23**, 283–437.